Chapter

Fabrication and Characterization of Cobalt-Pigmented Anodized Zinc for Photocatalytic Application

Judith Chebwogen and Christopher Mkirema Maghanga

Abstract

Population growth and urbanization have led to water scarcity and pollution, which is a health hazard not only to humans but also to the ecosystem in general. This has necessitated coming up with ways of treating water before consumption. Photocatalysis has proved to be one of the most promising cheap techniques that involve chemical utilization of solar energy. TiO_2 widely used in photocatalysis absorbs a narrow range of the solar spectrum compared to *ZnO*. In this regard, this study aimed at preparing and optimizing cobalt-pigmented *ZnO,* which is applicable in photocatalytic water treatment. The objectives in this study were to fabricate zinc oxide (*ZnO*) thin films by anodization, pigment the fabricated films with varying cobalt concentrations, characterize the fabricated films optically, and investigate the cobalt-pigmented *ZnO*'s performance in the methylene blue degradation under UV light irradiation. Mirror-polished zinc plates were sonicated in ethanol and rinsed. Anodization was done at room temperature in 0.5 M oxalic acid at a constant voltage of 10 V for 60 min, and cobalt electrodeposited in the films. Post-deposition treatment was done at 250°C. Optical properties of the films were studied using a UV-VIS-NIR spectrophotometer in the solar range of 300–2500 nm. The photocatalytic activity of the fabricated films was studied in methylene blue solution degradation in the presence of UV light irradiation for 5 h. Cobalt pigmenting was observed to reduce reflectance and optical band gap from 3.34 to 3.10 eV indicating good photocatalytic properties. In this study, *ZnO* film pigmented with cobalt for 20 s was found to be the most photocatalytic with a rate constant of 0.0317 h^{-1} and hence had the optimum cobalt concentration for photocatalytic water treatment. This can be applied in small-scale water purification.

Keywords: photocatalysis, anodization, zinc oxide, pigmenting, optical properties

1. Introduction

Contaminated waste water from industries, refineries, agriculture run-off, domestic and sewage water contain organic pollutants that are not only harmful to human but also the ecosystem in general. This calls for the need to treat water before discharge to the environment. Some of the water treatment methods used are reverse osmosis, sedimentation, filtration, distillation, coagulation and flocculation, chlorination, photocatalysis and aeration. According to Ref. [1], photocatalytic

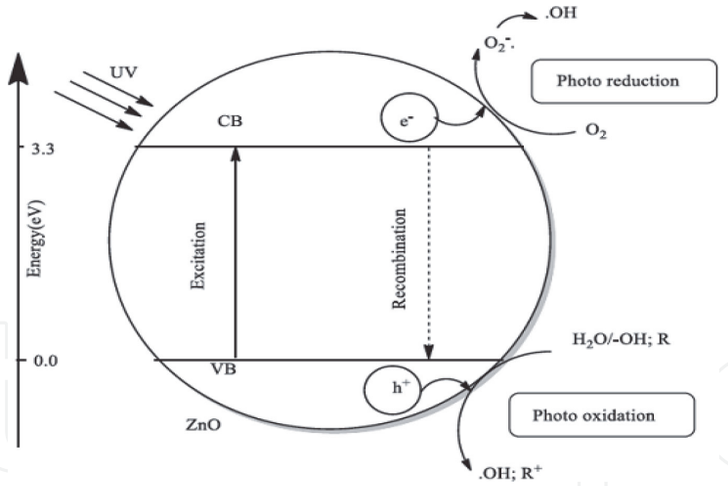

Figure 1.
Photocatalyst e− and h+ generation and their possible reactions in aqueous solutions [2].

water treatment has proved to be one of the most promising ways of purifying waste water. This technique degrades the hazardous organic pollutants in water by chemically utilizing solar energy. It involves the excitation of electrons from the valence band to the conduction band of a semiconductor by a radiation with sufficient energy. The photogenerated electrons and holes react with oxygen and hydrogen in water respectively to form superoxide and hydroxyl radicals as illustrated in **Figure 1**.

Photocatalytic water treatment is preferred because it is efficient, simple, possible to use solar light thus reusable and also capable to mineralize pollutants into products which are environment friendly [3]. Photocatalysis is also applied in air purification, in antibacterial action, hydrogen evolution through water splitting, designing self-cleaning surfaces, sterilization and photo electrochemical conversion. In these applications, semiconductors are used as photocatalysts.

Some of the attractive photocatalysts applied in photocatalytic degradation are Titanium dioxide (TiO_2), zinc oxide (ZnO), tin oxide (SnO_2). Iron (iii) oxide (Fe_2O_3), Vanadium (v) oxide and niobium pentoxide (Nb_2O_5) have also been reported by [4]. TiO_2 is the most studied and applied in photocatalysis because of its structural stability, nontoxicity and effectiveness according to [5, 6]. Its only drawback as compared with ZnO is that it absorbs a narrow range of the solar spectrum yet they have similar band gap energies, [7]. In addition, ZnO is readily available and cheaper than TiO_2.

2. Zinc oxide (ZnO) properties and applications

ZnO is an n-type direct wide band gap semiconductor whose crystals exist in hexagonal wurtzite, zincblende and rock salt structures but the most common structure is hexagonal wurtzite because it is stable. Its band gap energy is about 3.37 eV at room temperature, and it has a high exciton energy of 60 meV.

According to [8], *ZnO* photocatalysis is influenced by its direct band gap and large free exciton binding energy (60 meV). ZnO also possess unique properties like photosensitivity, nontoxicity, environmental stability and good optical and electrical properties. These properties according to [9] have attracted much interest in varied applications. It also has high electron mobility, good thermal conductivity and transparency. All these properties make *ZnO* a promising material in several semiconductor applications including designing of transparent thin film transistors,

light emitting diodes (LEDs), heat protecting windows and transparent electrodes in liquid crystal displays. They are also vital in applications like antibacterial use as reported by [10], dye sensitized solar cells by [11] gas sensors by [12] and photocatalysis as reported by [13].

2.1 ZnO photocatalytic water treatment

In photocatalytic water treatment, light energy greater than that of *ZnO* band gap illuminated on its surface excites electrons from its valence band to the conduction band leaving behind holes in the valence band. The excited electrons then interact with the surrounding oxygen to form superoxide radicals $\left(O_2^{-*}\right)$ while holes interact with water to form hydroxyl radicals (HO^*). These radicals react with the organic compounds dissolved in water decomposing them to water and carbon (IV) oxide. Photocatalytic water treatment process can be summarized using the equations, [14]:

$$ZnO + hv \rightarrow e_{cb}^{-} + h_{vb}^{+} \quad (1)$$

$$h_{vb}^{+} + H_2O \rightarrow H^{+} + HO^{*} \quad (2)$$

$$e_{cb}^{-} + O_2 \rightarrow O_2^{-*} \quad (3)$$

$$O_2^{-*} + H^{+} \rightarrow HO_2^{*} \quad (4)$$

$$HO_2^{*} + HO_2^{*} \rightarrow H_2O_2 + O_2 \quad (5)$$

$$H_2O_2 + e_{cb}^{-} \rightarrow HO^{*} + HO^{-} \quad (6)$$

$$H_2O_2 + hv \rightarrow 2HO^{*} \quad (7)$$

$$R + HO^{*} \rightarrow CO_2 + H_2O \quad (8)$$

Figure 2 illustrates how *ZnO* photocatalysis degrades organic pollutants.

ZnO photocatalytic activity is limited by its wide band gap property which makes it active only in the UV region of the solar spectrum [15]. This can be enhanced by doping or pigmenting it with a transition metal or nonmetal where the impurity added reduce the band gap consequently expanding its response to solar radiation. The preferred metal for pigmenting ZnO is Cobalt which has an ionic radius (0.745 Å) close to that of Zinc (0.74 Å) as stated by [16].

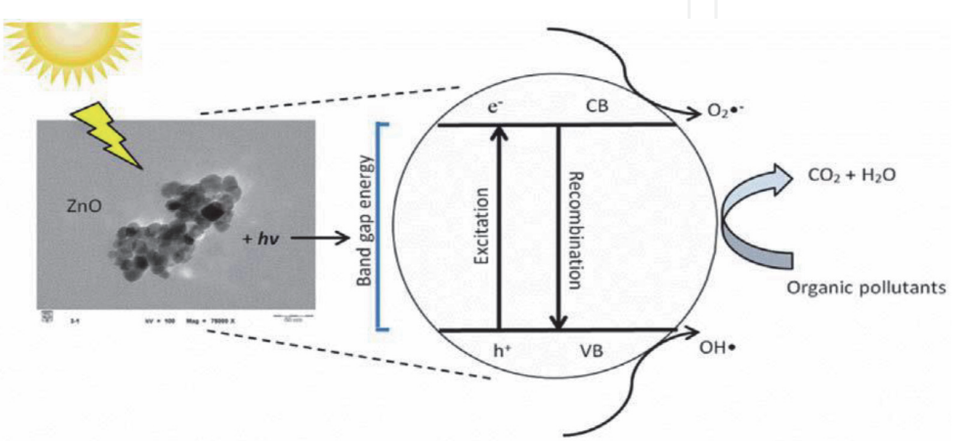

Figure 2.
Diagram showing ZnO *photocatalytic mechanism [13].*

3. Fabrication of zinc oxide thin films and nanostructures

Several techniques have been adopted in ZnO synthesis into different morphologies. These include spray pyrolysis, hydrothermal method, Radio Frequency (RF) and Direct Current (DC) magnetron sputtering, sol-gel and electrochemical anodization. The technique used determines the ZnO nanostructure formed. These nanostructures can be nanowires, nanoflowers, nanobelts and nanoparticles. ZnO thin films can also be fabricated using these techniques.

The choice of the technique in designing ZnO thin films is determined by the quality of the films required, simplicity, fabrication time and cost among others. In the synthesis of ZnO thin films, [17] acknowledged electrochemical anodization as a simpler route to design thin films. This technique is cheap. Simple and affordable.

3.1 Anodization

This is a simple two electrode configuration which involves a working electrode (anode) and a counter electrode (cathode) dipped in an electrolyte. A constant direct current passed through the electrodes results in the formation of a thin oxide layer on the surface of certain metals. The schematic diagram is as illustrated in **Figure 3**.

In this method of fabrication, several parameters like electrolyte temperature, inter-electrode spacing, electrolyte concentration, applied voltage and anodizing time should be controlled since they not only affect the nanostructure formation but also the surface density. While the type of electrolyte used determine the shape of the nanostructure, electrolyte concentration, anodizing time and the applied voltage influence the nanostructure density.

In the formation of ZnO thin films by anodization, Zinc metal is the working electrode (anode) and any inert material is the counter electrode (cathode). A constant current is passed from a power supply through the electrodes which results in redox reactions. These reactions are expressed as:

At the cathode:

$$2H^+ + 2e^- \rightarrow H_2 \tag{9}$$

At the anode:

$$\mathrm{Zn} \rightarrow Zn^{2+} + 2e^- \tag{10}$$

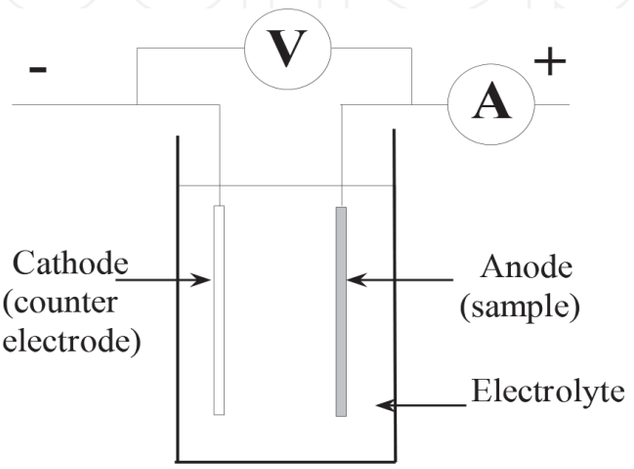

Figure 3.
Schematic diagram for the experimental setup for anodization [18].

$$Zn^{2+} + 2OH^{-} \rightarrow Zn(OH)_2 \tag{11}$$

$$Zn(OH)_2 \rightarrow ZnO + H_2\,O \tag{12}$$

4. Experiment

ZnO thin films were fabricated by anodizing about 99% pure ultrasonically cleaned Zinc metal in 0.5 M magnetic stirred Oxalic acid electrolyte at room temperature (300 K) for 60 min. Electric current was passed through the zinc metal (working electrode) and graphite (counter electrode) at a constant voltage of 10 V. The anodized films were rinsed in distilled water and then left to dry in air. This led to the formation of a white anodic film on the surface of Zinc metal. The experiment setup for anodizing Zinc is shown in **Figure 4**.

Varying Cobalt concentrations were incorporated into ZnO films by electrodeposition method using 0.5 M Cobaltous (II) sulphate solution as the Cobalt source. This was done by passing alternating current from a 20 V source through the Cobaltous (II) sulphate solution containing ZnO working electrode and graphite counter electrode for 10, 20, 30, 40, 50 and 60s. The films were then rinsed and left to dry in air. Heat treatment was done in a Carbolite 301 temperature controller at 523 K for 2 h.

The amount of Cobalt deposited in ZnO films at different deposition times was obtained using the Faraday's law of electrochemistry which is expressed mathematically as [19]:

$$m = \left(\frac{Q}{F}\right)\left(\frac{M}{z}\right) \tag{13}$$

where m is the mass of Cobalt deposited expressed in grams, Q is the charge in coulombs passed through ZnO, F is the Faraday constant (96485.33289 $Cmol^{-1}$), M represents the molar mass of Cobalt expressed in grams mol^{-1} and z is the valency number of Cobalt. Q is given by the product of current passed and time in seconds (Q = It) where the current passed is 2.18 A.

Optical characterization was done using PERKIN ELMER UV/VIS/NIR Lambda 19 spectrophotometer equipped with an integrating sphere which can be used to measure the absorbance, transmittance and reflectance of the films.

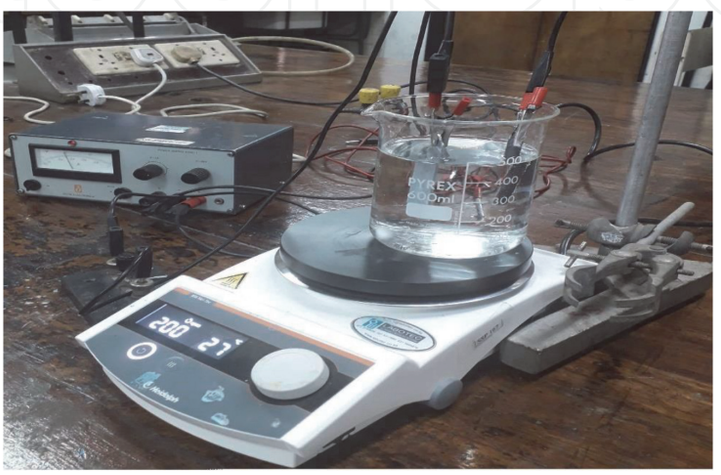

Figure 4.
Plate showing the experimental setup for anodizing zinc metal.

This spectrophotometer was set to measure the reflectance of the films in the solar range 300 nm $< \lambda <$ 2500 nm against a barium sulphate reference standard.

The photocatalytic activity of unpigmented and Cobalt-pigmented *ZnO* thin films was studied in the degradation of aqueous methylene blue solution which is the simulated pollutant under UV light. The UV source composed of a UV cabinet with a UV lamp of wavelength 366 nm, 2 $\times$ 6 W irradiation power and methylene blue absorbance was measured using Optima SP-3000nano UV-VIS spectrophotometer. 60 ml of methylene blue with 10 ppm concentration was put in a petri dish and placed in the dark for 60 min to allow for adsorption-desorption equilibrium.

The petri dish and its contents were then transferred into the UV cabinet and illuminated for 5 h at ambient temperature. 1 ml of the degrading solution was drawn at 30 min intervals and its absorbance directly measured at 664 nm using the UV-VIS spectrophotometer. The absorbance recorded in this case was directly proportional to methylene blue concentration. This was revealed by a calibration curve plotted from standard methylene blue solutions of known concentrations prepared prior to the measurement. The calibration curve was used to obtain the concentration of methylene blue in the experiment with respect to absorbance.

4.1 Data analysis

Data was analyzed using SCOUT software which allows for analysis and simulation of optical spectra such as reflectance, transmittance and absorbance. This was done by fitting the measured experimental data into the simulated data in the software with the aid of different models. In this case, the models used are the Drude model for free carriers, harmonic oscillator to describe the atomic microscopic vibrations and Tauc Lorentz model to determine the band gaps of the films.

5. Results

A white ZnO thin film formed on Zinc electrode surface as a result of the redox reactions at the anode and cathode. The average film thickness as obtained from fitting of the experimental measured spectra into the simulated spectra using SCOUT software was 110 nm. **Figure 5** shows one of the obtained fitted spectra.

5.1 Reflectance spectra

The reflectance spectra of the fabricated films obtained from the spectrophotometer is shown in **Figure 6**.

As seen in the **Figure 6**, ZnO reflectance was affected by Cobalt pigmenting because Cobalt pigmented ZnO films had a lower reflectance than unpigmented ZnO. This decrease in reflectance may be attributed to darkening of the films when Cobalt concentration was increased. Lowered reflectance may also be as a result of the films becoming rough as Cobalt is deposited according to Ref. [20]. The more the Cobalt concentration, the rougher the films hence the decrease in the quantity of reflected light implying increased light absorption (absorbance).

5.2 Absorption coefficient

The absorption coefficient of the fabricated films was obtained from reflectance data of the films using the relation [21]:

$$R + T = e^{-\alpha d} \tag{14}$$

which yields

$$\alpha = \frac{1}{d} \ln \left[\frac{1}{R(\lambda)} \right] \tag{15}$$

where α is the absorption coefficient, d is the film thickness and $R(\lambda)$ is reflectance as a function of wavelength. **Figure 7** shows the variation of the absorption coefficient of the films with wavelength.

From the figure, it was observed that there is a sudden increase in the absorption coefficient at shorter wavelengths about 348 nm. This peak corresponds to ZnO absorption edge indicating that ZnO absorbs at short wavelengths in the UV region of the solar spectrum. It was also observed that Cobalt pigmenting affected the absorption coefficient since an increase in the Cobalt concentration led to an increase in the absorption coefficient. This may be attributed to the decrease in

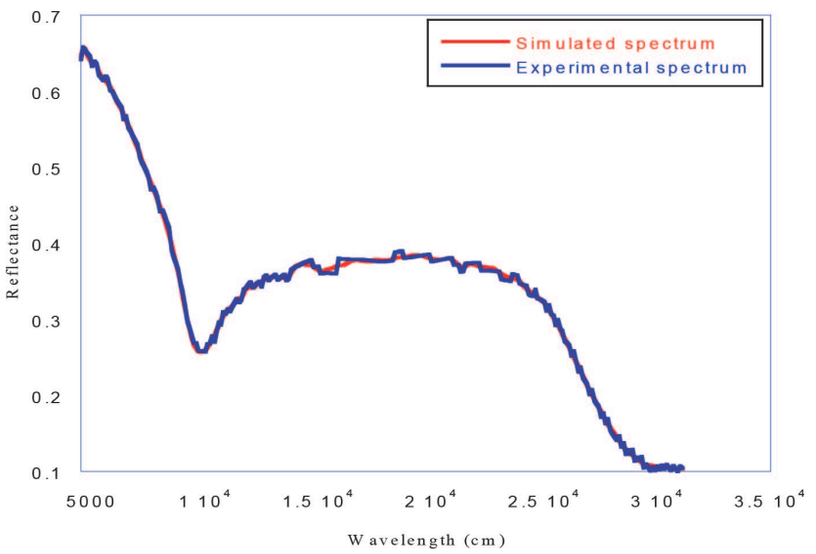

Figure 5.
Illustration of fitting of experimental to simulated spectra.

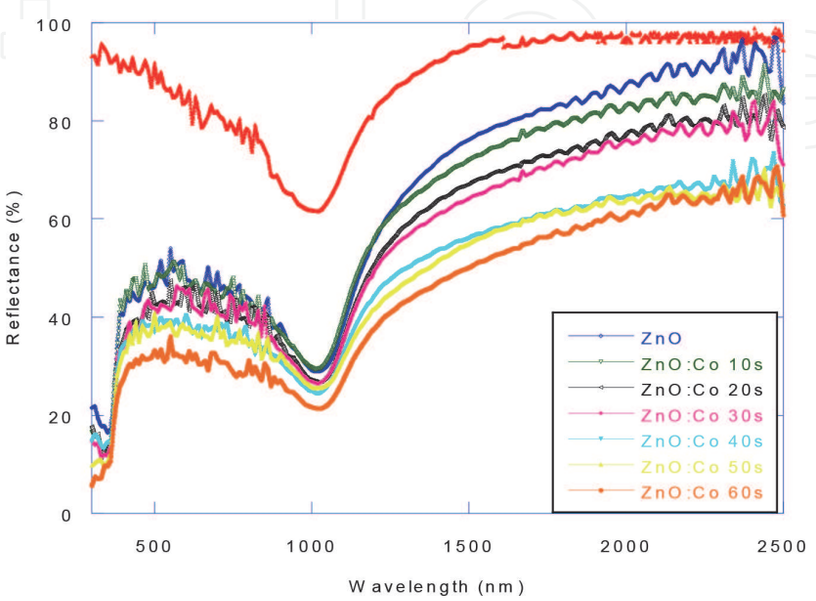

Figure 6.
Measured reflectance for zinc and the ZnO *films with different cobalt concentrations.*

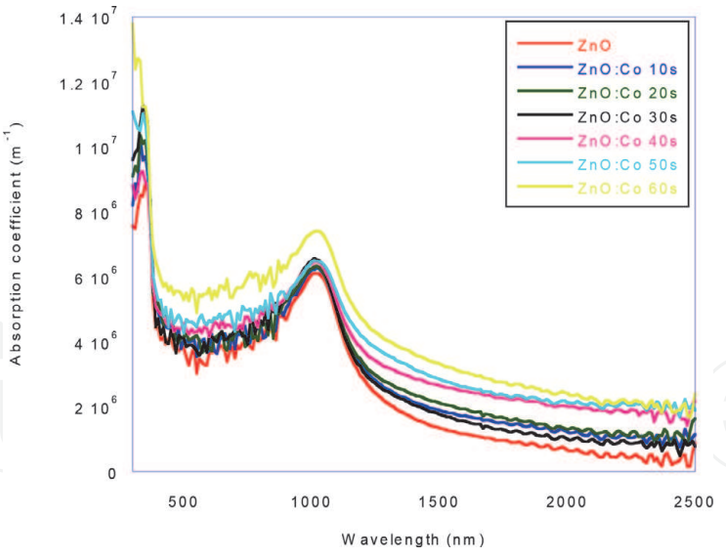

Figure 7.
Variation of absorption coefficient of the films with wavelength.

reflectance of the films as Cobalt concentration was increased. According to Ref. [22], the content of pigment in a film affects its absorption. Another peak was observed at about 1000 nm which shows absorption resulting from interband transition in the Zinc substrate [23].

5.3 Optical band gap

ZnO is a direct band gap semiconductor whose band gap can be obtained from a plot of $(\alpha h\nu)^2$ versus energy in eV. **Figure 8** shows the band gaps of the fabricated films.

The band gaps of the films ranged from 3.34 to 3.10 eV for pure ZnO and ZnO: Co 60s films respectively. The fabricated pure *ZnO* films had a band gap of 3.34 eV which is similar to the preceding work done in Ref. [24] who also found 3.34 eV. The gradual decrease observed as Cobalt was introduced into the *ZnO* films in different amounts is associated with the red shift of the absorption edge as observed in the reflectance spectra.

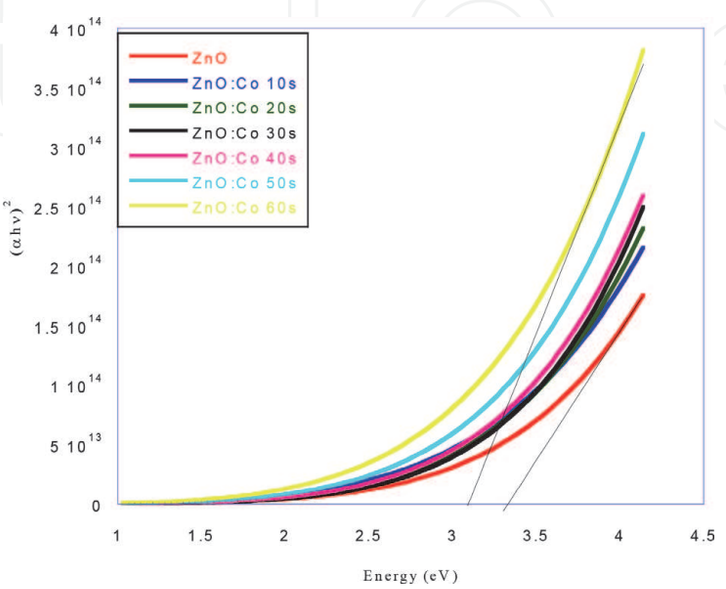

Figure 8.
Graph showing the band gap analysis of the fabricated films.

In Refs. [25–27], a gradual decrease in ZnO band gap with Cobalt pigmenting is also reported. They attributed the decrease to sp-d exchange interactions between the d electrons of Cobalt and *ZnO* conduction band electrons once the Cobalt ions substitute the Zinc ions in the crystal lattice. It was also stated that High Cobalt concentration led to the wavefunctions of the electrons in the Cobalt atoms overlapping as the Cobalt density increases resulting in the formation of an energy band by the overlapping forces consequently reducing the gap.

5.4 Photocatalytic degradation of methylene blue

In the investigation of photocatalytic degradation of methylene blue solution, the pseudo-first order kinetic model was used which according to [28] enables quantification of the photocatalytic activity of samples. This model involves the presentation of raw data as integral data. The performance of the pure and some of the Cobalt pigmented *ZnO* films was as shown in **Figure 9**. Methylene blue degradation without catalyst was used the control experiment.

From the figure, it is observed that the rate at which methylene blue with catalyst degraded was faster than that without the catalyst. Also, Cobalt pigmenting increased the degradation rate which may be attributed to the decrease in the optical band gap resulting from the red shift which was observed in the reflectance spectra. This shift resulted in more electrons gaining kinetic energy consequently moving to the conduction band to take part in the degradation process.

ZnO:Co 20s is had a higher rate of degradation with its degradation rate of 0.0317 h^{-1} obtained using the relation [28]:

$$-\ln\left(\frac{C}{C_0}\right) = kt \tag{16}$$

where k is the degradation rate constant given by the slope of the graph.

Heavy Cobalt content however lowered the methylene blue degradation rate. This may be attributed to the fact that excess metal pigment covered the active sites

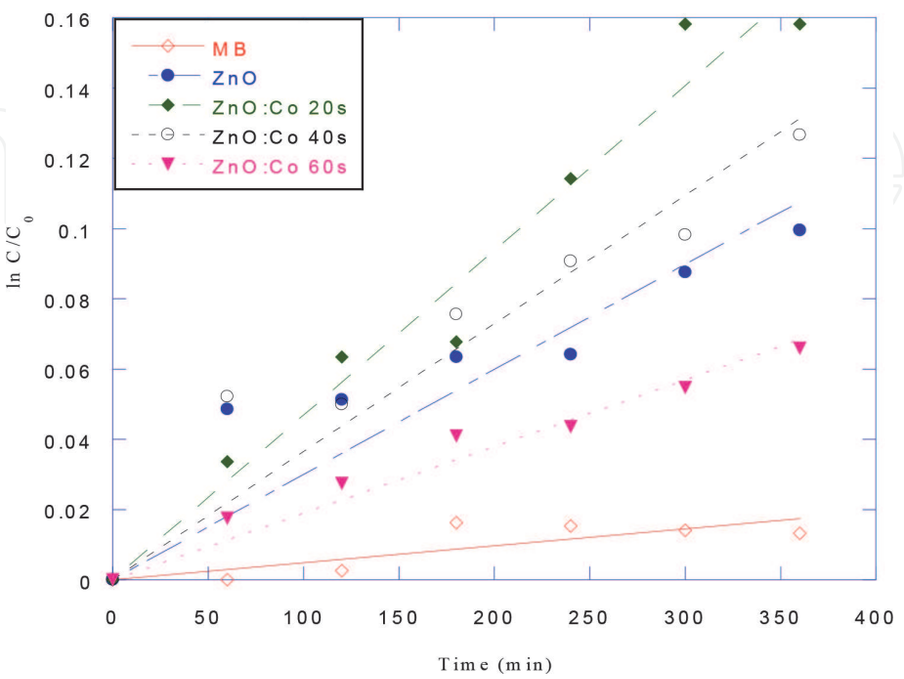

Figure 9.
A graph of ln (C/C_o) versus time in minutes for sampled films.

of the *ZnO* catalyst lowering its activity. It may also be due to the generation of the impurity levels deep in *ZnO* band gap which acted as recombination centers for the photogenerated electrons.

6. Conclusion

- ZnO thin films were successfully fabricated by anodization. The film formed was white in color.
- Reflectance of the ZnO films decreased with increase in cobalt content; hence, the increase in absorption on pigmenting is attributed to the films becoming rougher with increase in cobalt concentration.
- The band gap of ZnO changed from 3.34 eV for unpigmented to 3.10 eV for the most pigmented film.

Acknowledgements

The authors acknowledge the International Science Programme of Uppsala University who funded the research and the Departments of Chemistry and Physics of The University Of Zambia for their laboratory facilities under the auspices of Materials Science and Solar Energy Network for Eastern and Southern Africa (MSSEESA).

Author details

Judith Chebwogen* and Christopher Mkirema Maghanga
Kabarak University, Nakuru, Kenya

*Address all correspondence to: judithkoskey86@gmail.com

References

[1] Hoffmann MR, Martin ST, Choi W, Bahnemann DW. Environmental applications of semiconductor photocatalysis. Chemical Reviews. 1995; **1**:69-96

[2] Irani M, Mohammadi T, Mohebbi S. Photocatalytic degradation of methylene blue with ZnO nanoparticles; a joint experimental and theoretical study. Journal of the Mexican Chemical Society. 2016;**60**(4):218-225

[3] Prihod'ko RV, Soboleva NM. Photocatalysis: Oxidative processes in water treatment. Journal of Chemistry. 2013

[4] Vinu R, Madras G. Environmental remediation by photocatalysis. Journal of the Indian Institute of Science. 2012; **90**(2):189-230

[5] Fujishima A, Rao TN, Tryk DA. Titanium dioxide photocatalysis. Journal of Photochemistry and Photobiology C: Photochemistry Reviews. 2000;**1**(1): 1-21

[6] Klosek S, Raftery D. Visible light driven V-doped TiO_2 photocatalyst and its photooxidation of ethanol. The Journal of Physical Chemistry B. 2001; **105**(14):2815-2819

[7] Lizama C, Freer J, Baeza J, Mansilla HD. Optimized photodegradation of Reactive Blue 19 on TiO_2 and ZnO suspensions. Catalysis Today. 2002;**76** (2-4):235-246

[8] Huang MH, Mao S, Feick H, Yan H, Wu Y, Kind H, et al. Room-temperature ultraviolet nanowire nanolasers. Science. 2001;**292**(5523):1897-1899

[9] Kong XY, Wang ZL. Spontaneous polarization-induced nanohelixes, nanosprings, and nanorings of piezoelectric nanobelts. Nano Letters. 2003;**3**(12):1625-1631

[10] Xie Y, He Y, Irwin PL, Jin T, Shi X. Antibacterial activity and mechanism of action of zinc oxide nanoparticles against *Campylobacter jejuni*. Applied and Environmental Microbiology. 2011; **77**(7):2325-2331

[11] Agus SG, Irmansyah I, Akhiruddin M. Dye-sensitized solar cell based on flower-like ZnO nanoparticles as photoanode and natural dye as photosensitizer. Журнал нано-та електронної фізики. 2016;**8**(2):02012-02011

[12] Madhusoodanan KN, Vimalkumar TV, Vijayakumar KP. Gas sensing application of nanocrystalline zinc oxide thin films prepared by spray pyrolysis. Bulletin of Materials Science. 2015;**38** (3):583-591

[13] Ong CB, Ng LY, Mohammad AW. A review of ZnO nanoparticles as solar photocatalysts: Synthesis, mechanisms and applications. Renewable and Sustainable Energy Reviews. 2018;**81**: 536-551

[14] Goswami DY. Advances in Solar Energy: An Annual Review of Research and Development. Vol. 10. Boulder: ASES; 1995. pp. 165-209

[15] Iqbal J, Jilani A, Hassan PZ, Rafique S, Jafer R, Alghamdi AA. ALD grown nanostructured ZnO thin films: Effect of substrate temperature on thickness and energy band gap. Journal of King Saud University-Science. 2016;**28**(4):347-354

[16] Woo HS, Kwak CH, Chung JH, Lee JH. Co-doped branched ZnO nanowires for ultraselective and sensitive detection of xylene. ACS Applied Materials & Interfaces. 2014;**6**(24):22553-22560

[17] Voon CH, Derman MNB, Hashim U, Foo KL. Effect of anodizing voltage on the formation of porous anodic alumina on Al-0.5 wt% Mn alloys. Advanced Materials Research. 2014;**925**:455-459

[18] Nemes D, Moldovan V, Bruj E, Jumate N, Vida-Simiti I. Porous anodic alumina films obtained by two step anodization. Bulletin of the Transilvania University of Brasov. Series I: Engineering Sciences. 2011;**4**(2):75

[19] Bhattacharyya B. Electrochemical Micromachining for Nanofabrication, MEMS and Nanotechnology. Massachusetts: William Andrew Applied Science Publishers, Imprint of Elsevier Inc.; 2015. p. 270

[20] Yousif AA, Habubi NF, Haidar AA. Nanostructure zinc oxide with cobalt dopant by PLD for gas sensor applications. Journal of Nano- and Electronic Physics. 2012;**4**(2):02007

[21] Benno G, Joachim K. Optical properties of thin semiconductor films; 2003

[22] Bakr NA, Salman SA, Shano AM. Effect of co doping on structural and optical properties of NiO thin films prepared by chemical spray pyrolysis method. International Letters of Chemistry, Physics and Astronomy. 2015;**41**:15-30

[23] Palik ED, editor. Handbook of Optical Constants of Solids. Vol. 3. Academic Press; 1998

[24] Yildirim OA, Arslan H, Sönmezoğlu S. Facile synthesis of cobalt-doped zinc oxide thin films for highly efficient visible light photocatalysts. Applied Surface Science. 2016;**390**:111-121

[25] Kao CY, Liao JD, Chang CW, Wang RY. Thermal diffusion of Co into sputtered ZnO:Co thin film for enhancing visible-light-induced photo-catalytic activity. Applied Surface Science. 2011;**258**(5):1813-1818

[26] Sutanto H, Wibowo S, Arifin M, Hidayanto E. Photocatalytic activity of cobalt-doped zinc oxide thin film prepared using the spray coating technique. Materials Research Express. 2017;**4**(7):076409

[27] Borhani Zarandi M, Amrollahi Bioki H. Effects of cobalt doping on optical properties of ZnO thin films deposited by sol–gel spin coating technique. Journal of Optoelectronical Nanostructures. 2017;**2**(4):33-44

[28] Gajbhiye SB. Photocatalytic degradation study of methylene blue solutions and its application to dye industry effluent. International Journal of Modern Engineering Research. 2012;**2**(3):1204-1208